

Glass-aluminium bonded joints; testing, comparing and designing for the ATP

S.A.J. de Richemont

TNO Building and Construction Research, Delft, sabine.derichemont@tno.nl

F.A. Veer

Faculty of Architecture, Delft University of Technology, f.a.veer@tudelft.nl

This article presents the research to the bonded joints of the All Transparent Pavilion (ATP), an experimental project built in November 2004 at the faculty of Architecture in Delft. The pavilion is designed to use structural glass elements, bonded with Delo Photobond GB 368, a photo-catalytic transparent adhesive. To avoid bonding on-site and to allow disassembly, the joints were designed as aluminium pieces, bonded to the glass.

Some joints of the ATP failed during construction. The tolerances for assembling the two aluminium parts were too small, and joints had to be forced together. The Delo Company suggested an alternative adhesive: The GB 350, a rubber modified version and supposedly tougher version of the GB 368.

The research consisted of two parts: First, the mechanical behaviour of GB 368 and GB 350 were compared, and secondly designing an improved solution for the glass-aluminium bonded joint between the main beam and purlin. This article focuses on the mechanical behaviour of GB 368 and GB 350.

Three types of tests were performed: tensile tests, low cycle fatigue tests and fracture toughness tests. Results show that both adhesives have low damage tolerance and are therefore sensitive to damage during assembly. Although the GB 350 was recommended by the Delo company because it was designed to resist impact loads, results show the improvement is not enough. The GB 350 is better in static tests, but the fatigue tests show great scatter and the fracture tests show peeling of the adhesive from the adherent surface. Given this, the GB 350 should be more susceptible to corrosion.

Key words: Glass, adhesives, joints

1 Introduction

This article presents the experimental results for strength of glass-aluminium bonded joints, which was part of a graduation project for the faculty of Architecture at the University of Delft. Glass gains popularity as a structural material for transparent buildings and is used by architects because of its transparency and smooth surface. Although there are many largely transparent buildings, most of them are concrete or steel structures with a glass facade to simulate a light and transparent object. In order to substitute the concrete or steel parts with transparent elements, the research of the past decades has focused on transparent joints and transparent structural parts. Glass is a material which can be used for transparent structural elements, but is very brittle. It fails without visual warning into separate pieces and loses its carrying capacity. The research group at the faculty of architecture has been able to develop glass elements with a more ductile mode of failure. By laminating and reinforcing glass plates, a glass beam can be obtained which keeps its strength after cracking.

The joints for glass structures have to be safe too. Several techniques have been developed for joining glass elements, such as soldering, welding and adhesively bonding. The bolted joint is the most common type of connecting two pieces of glass. Unfortunately this way of joint has several disadvantages, the most important of which is that the strength of glass is reduced by drilling holes. Adhesive joints are considered less secure as there are risks of surface contamination prior to bonding. Moreover adhesive joints require complicated manufacturing while there is also a long term risk of corrosion by moisture. However several new types of adhesives have been developed which can compete with bolted joints [2].

Another problem with bolted joints is the necessity of tempering the glass to increase the local strength. This contradicts with the demand for safe structures as tempered glass fails explosively into little pieces. Laminated reinforced annealed float glass can meet the safety requirements as a more ductile failure mode is possible.

Adhesively bonded joints were used for the All Transparent Pavilion (ATP), an experimental project of the research group for transparent architecture at TU Delft, which was built to show the progress that has been made in 10 years (Chapter 1). During the building of the ATP, bonded joints between the main beam and purlins failed as the adhesive could not resist the impact loads that were needed to force the joints. First part of the research was to design an alternative joint for the ATP, which would not give assembly problems as occurred before (Chapter 2). Second part was comparing the fracture behaviour of another adhesive (GB 350) with the originally used adhesive (GB 368). The GB 350 was recommended by the Delo company as a reaction to the failing joints. In order to increase the knowledge of the failure behaviour of both adhesives, tests were performed on tensile strength, low cycle fatigue strength and fracture toughness (3).

2 All Transparent Pavilion

In November 2004, the All Transparent Pavilion (ATP) was an engineering project of the Zappi research group at the Faculty of Architecture, Delft, [1]. In the past ten years, the two main goals of the Zappi project were to produce methods for the design of transparent elements with safe failure behaviour (a more ductile failure mode which gives a visual warning prior to collapse) and to develop new concepts for transparent structures.

The adhesive used for bonding glass of the ATP, was Delo Photobond GB 368. This adhesive has several advantages. It is suitable for large areas, easy to apply on glass, is photocatalytic and allows controlled curing [2].

2.1 Design

The 9m x 9m roof was supported by 3 main beams with a length of 7,2m and 2 x 7 purlins with a length of 3,6m. Laminated glass 1,5 m high columns, standing on a 1,5m steel foot were used to support the main beams. The stability was provided by the roof and the façade walls which were made out of 3,6m high panels of 1,2 m and 1,5m width.

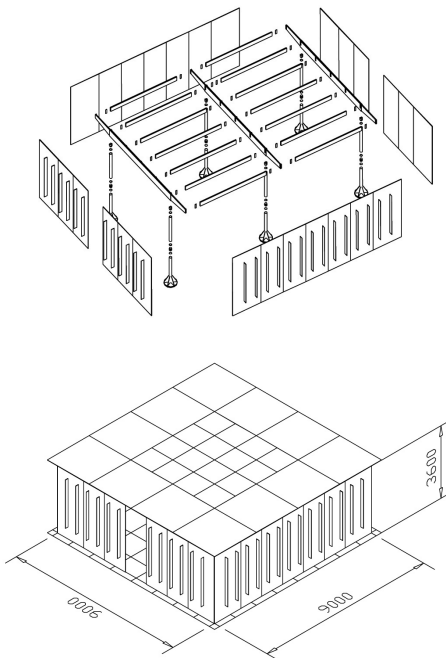


Figure 1: Exploded view and 3d view of the design of the ATP, from [1]

2.2 *Joint failure*

The joints between the main beams and the purlins of the ATP were realized by bonding pieces of aluminium onto the separate structural parts, which could slide into each other. To ensure stability of the ATP, the joints had to be rigid [1] which was achieved by keeping the tolerances of the joints very small. Unfortunately, these small tolerances resulted in assembly problems of joints, while there was no room to compensate for production deviations. During assembling, the joints of the main beams and the purlins failed due to temporary and locally applied impact loading and the effect of peel stresses in the joint.



Figure 2: *Low cycle impact loading of the joints*

As a reaction to the problems encountered, the Delo company recommended the use of another (improved) photobond adhesive which was supposed to withstand impact loads better than the original adhesive. The research presented in the following chapters was to solve the problem of failing joints. This by increasing the knowledge of the failure behaviour of both adhesives and designing an alternative joint which reduces peel stresses.

3 **Design of the joint**

The design challenge was to make a joint for the All Transparent Pavilion. The joint had to be dismantlable as it is part of a pavilion and not a permanent building. Secondly, a rigid joint was demanded in order to transfer bending moments. Thirdly, the joint had to have sufficient tolerances for easily aligning the elements and building the pavilion. The design process included research of the construction of the ATP and various alternative joints using finite element method programme Diana, but this is not covered in this article.

The final design, as can be seen in Figure 3, existed of small pieces of aluminium which can

easily slide into each other. Two C-shaped aluminium pieces were bonded to the main beam, one T-shaped aluminium piece was bonded between the glass plates of the purlin. The tolerances are large enough to provide easy assembling. Bolts are used in order to make a rigid joint. Although aluminium is not a transparent material, it has great benefits compared to glass and other transparent materials (such as PMMA) as it is ductile, easily machined and thus suitable for joints which can be disassembled.

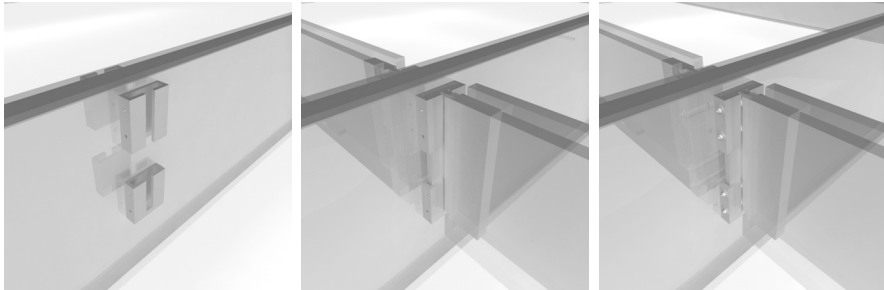


Figure 3: Assembling the purlin to the main beam

4 Experimental tests

In this work two types of adhesives are studied, Delo Photobond GB 368 and Delo Photobond GB 350. The 368 adhesive is a strong viscous adhesive. The 350 is a less viscous rubber modified version [4]. The rubber modification should give better absorption of impact loads. Both adhesives are transparent with a Young's modulus of 900 MPa.

For comparing the failure behaviour of these two adhesives, three types of tests were performed: tensile testing, low cycle fatigue testing and fracture toughness testing.

4.1 Tensile and low cycle fatigue testing

Four different types of specimen were used. The first, specimen A, is an asymmetric butt strap specimen as used before [3]. This specimen is illustrated in Figure 4 and is used to test the adhesive in shear. The main problem with this type of specimen is that it has four adhesive joints. Even in the asymmetric specimen there are two (out of four) joints, that are initially stressed equally. As one side fails it becomes less stiff and thus increases the load on the second side. Although specimen is convenient and easy to manufacture, the fact that it has two failure zones is a major disadvantage.

The second specimen, specimen B, is based on the double butt strap specimen but uses a milled aluminium piece which replicates $\frac{3}{4}$ of the specimen on which a single glass sheet is bonded asymmetrically. Although this specimen is time consuming to manufacture it has only a single

zone of failure. As the aluminium has the same Young’s modulus as the glass there are no additional stress concentrations compared to specimen type A. The 50 μm thin adhesive layer should have no effect on the overall stiffness.

Specimen C is a linear direct tension specimen. It loads the adhesive joint in direct tension and is easy to manufacture. A major problem is illuminating the joint to obtain proper and even curing. In addition this specimen has two zones of failure.

Specimen D is based on specimen C but has an oversized piece of glass. Twisting of the bonding surfaces can be limited and the oversized piece allows better illumination and thus more even curing. It still has the major disadvantage of two joints that can fail. Manufacturing an asymmetric version of this specimen was tried but the problems in producing a consistently shaped glass centre piece for this proved insurmountable. Specimen sizes are given in Table 1. The specimen geometry used for the fatigue tests are the same as those of specimen B and D in the tensile tests.

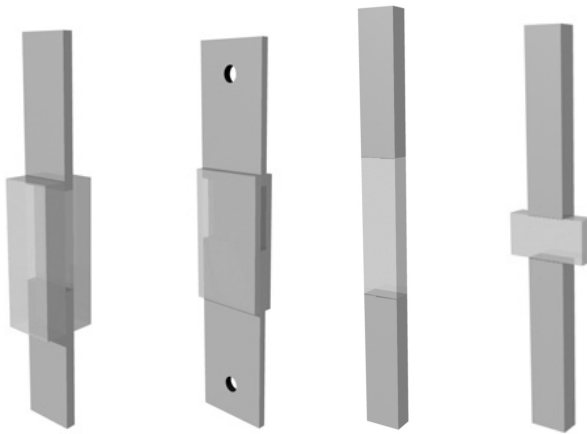


Figure 4: Specimens, from left to right: A, B, C and D

Table 1: Dimensions of specimens

Specimen type	Length of adhesive joint (mm)	Width of adhesive joint (mm)	Area of adhesive joint (mm ²)
A	6	40	2×240
B	5	40	200
C	30	15	450
D	30	15	450

4.2 Fracture toughness testing

For measuring the fracture energy G_{IC} of structural adhesive joints, the double cantilever beam (DCB) and the tapered double cantilever beam (TDCB) are the most commonly used types of specimens. In this work, the use of glass as an adherent makes it difficult to produce the complex geometry while retaining the ability to resist the bending moments.

As a result, the specimen type chosen for this study is based on a modified Compact Tension (CT) specimen. This type of specimen is often used to determine the fracture energy of metals and is simple to produce. The choice of a CT type specimen is validated by the fact that the Young's moduli of glass and aluminium are about the same. The fracture energy can be calculated by the same formula 1:

$$G_{IC} = \frac{12P^2a^2}{EB^2h^3} \quad (1)$$

in which P is the applied load [N], a the crack length [mm], E the E-modulus of the adhesive [MPa], B the thickness of the specimen [mm], and h the height of the specimen. [mm]

The plain strain fracture toughness can be obtained using formula 2

$$K_{IC} = \sqrt{G_{IC} * E} \quad (2)$$

in which G_{IC} is the critical energy release rate [N/mm] and E is the E-modulus of the adhesive [MPa]

Despite the easy geometry, two adjustments had to be made:

1. The maximum thickness of the available glass, was 20 mm. According to ASTM E399-05 standard [7] the specimen width and height for obtaining a plain strain situation should be determined by respectively $B = \frac{W}{2} \pm 0.010W$ and $\frac{1}{2}H = 0.6W \pm 0.005W$ in which W is the sample's width. As a consequence, the dimensions of the specimens would be 20 mm x 40 mm x 48 mm. This is very inconvenient in terms of manufacturing and increases the risk of a large standard deviation. Hence, the width and height of the specimens were enlarged to 100 mm and 100 mm respectively.
2. In a metallic CT specimen, a saw notch introduces the crack. In this research, it was not possible to make a saw notch after bonding the two pieces as this would cause significant damage. It is also not recommended to make only a saw cut prior to bonding as the adhesive is difficult to remove and affects the results. Therefore the geometry of the

specimen modified by tapering one edge. The angle had to be large enough to prevent interference of the residual adhesive.

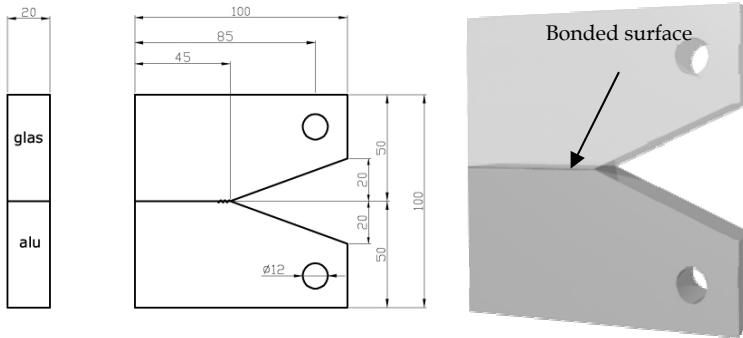


Figure 5: Specimen for fracture toughness tests.

4.3 Test set up

Specimens of all types were manufactured using proper safeguards such as using jigs to ensure proper positioning and springs to apply a constant and adequate force on the joint during curing. All specimens were illuminated for 5 times the required time to ensure complete and full curing.

All specimens were tested on a Zwick Z10 testing frame using Testexpert version 10 software. Tests were conducted in laboratory air at 20°C. Fatigue tests were conducted using block loading rather than sinusoidal loading. Block loading more closely resembles the repeated impact loading experienced in practice.

To ensure a sharp crack tip, the specimens for fracture toughness testing were notched using a sharp knife, in a method similar to that done by Riemslog on polymers [5]. In addition, a low cycle fatigue load was applied to half of the specimens of each series in order to obtain a sharp crack tip by allowing for a small amount of crack growth.

Force, displacement and time were recorded during the experiments. A standard displacement rate of 10 mm/minute was used for the fatigue tests and 1 mm/min for the tensile tests. In the fatigue tests the hold time, $t_{h,max}$, at maximum load was varied. The recovery time at minimum load, $t_{h,min}$, was also varied in some tests. Fatigue tests that lasted more than 15.000 cycles were stopped as the available machine time was limited.

The fatigue load for the fracture toughness specimens was set on +200 N to +700 N with 200 N/s, due to the danger of failure (by the brittleness of the adhesive), followed by a standard displacement rate of 0.25 mm/min.

5 Experimental results

5.1 Results of tensile tests

The results of the tensile test on the different types of specimens are given in Table 2. The mean is the result of at least 5 tests. There were no test results that deviated from the mean in such a way that they had to be neglected. The results show that although the single sided double butt strap specimen has the best strength and reasonable scatter leading to the assumption that this specimen is the most comparable.

Table 2: Results of tensile tests on different types of specimen

Specimen type	Adhesive type	Mean failure stress (MPa)	Standard deviation (% of average)
A	350	10.98	17
	368	9.87	32
B	368	15.7	16
C	350	10.93	12
	368	7.48	17
D	350	12.55	16
	368	10.42	16

5.2 Results of fatigue tests

Initially fatigue tests were conducted on all types of specimens. In further experiments only specimens B and D were tested, as it was clear the scatter for specimens A and C was far greater than for specimens B and D in initial tests. Table 3 gives an overview on test methods. Specimen B is used for testing the adhesive in shear and therefore M1 and M2 are expressed in τ . M3 and M4 are expressed in σ , since specimen D is used for fatigue testing normal to the bonding surface.

Results of specimens B and D are given in Table 4. It is clear that even these results have too much scatter for any meaningful statistical treatment. It should be noted from the data on specimen D that decreasing the frequency seems to increase the fatigue life. Apparently fatigue loading causes more damage than creep.

Figure 6 shows a plot of displacement against time for a fatigue test on specimen type B (shear) using photo bond 368 adhesive. The initial increase in displacement is due to the fact that the specimen is not clamped but held with pins. This displacement sets the pins in the grips. Any following changes are assumed to be the result of debonding.

Table 3: Overview of methods for fatigue tests

test method	τ_{\max} (MPa)	τ_{\min} (MPa)	$t_{h,\max}$ (s)	$t_{h,\min}$ (s)
M1	12.5	7.5	1	1
M2	7.5	2.5	1	1
	σ_{\max} (MPa)	σ_{\min} (MPa)	$t_{h,\max}$ (s)	$t_{h,\min}$ (s)
M3	8	1	2	10
M4	8	1	10	10

In which τ_{\max} , τ_{\min} , σ_{\max} , σ_{\min} are the maximum and minimum shear stress and maximum and minimum normal stress respectively and $t_{h,\max}$ and $t_{h,\min}$ are the hold times at maximum and minimum load.

Table 4: Results of fatigue tests

Specimen	B	B	D	D	D	D
Adhesive	368	368	350	350	368	368
Test method	M1	M2	M3	M4	M3	M4
number of cycles	9	1836	1	2	1	324
until failure	12	2035	41	28	25	7724
	61	8350	316	4514	1026	9753
	62	12650	719	13271		
	72	>15000				
	134					

A slight increase in maximum displacement can be observed during the test but only in the last three cycles before failure can any increase be observed. Figure 6 shows a detail of a single cycle of the middle part of the test. At the beginning of the cycle a small increase in displacement is observed. This presumably is the damage part of the cycle. The adhesive shows no visco-elastic flow or relaxation when the stress is reduced.

Figure 7 shows a single cycle of a test on specimen D (tension) using glass bond 368 adhesive. This test used holding times of 10 seconds at maximum and minimum load. Again there is only a displacement increment at the beginning of the test and no visco-elastic flow or relaxation. The adhesives seem to be strong, rigid and brittle. Low toughness of the adhesives seems to cause failure at limited damage. As a consequence, failure can occur in just a few cycles if enough damage exists at the start of the test. The enormous spread in fatigue life supports this assumption.

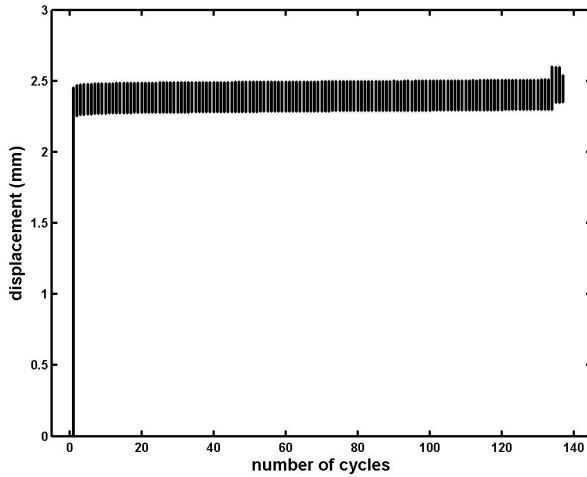


Figure 6: Plot of displacement against cycles for fatigue test on specimen B

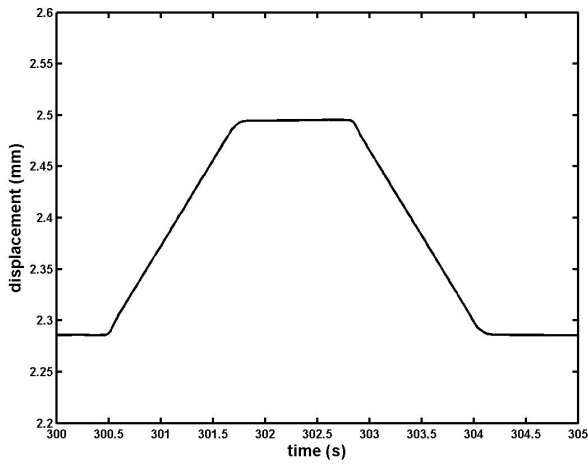


Figure 7: Detail of Figure 4

5.3 Results of fracture toughness tests

The results of the fracture toughness tests are given in Tables 5 and 6. The first specimens were tested with a low cycle fatigue load prior to fracture testing. Some specimens did not give usable results because the glass failed before the adhesive. Specimen 5 and 6 of GB 350 failed during fatigue loading. As a consequence, the fatigue load for the other GB 350 specimens was decreased to +200 N and +500 N. Specimen 8 of the GB350 series also failed during fatigue loading, even with lower load.

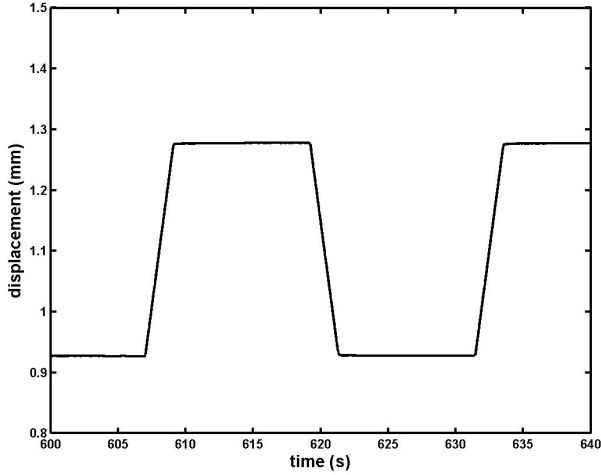


Figure 8: Plot of displacement against time for single cycle of fatigue test on specimen type D with long holding time and long relax time.

Table 5: Results for GB 368 bonded specimens

Specimen number	a_c [mm]	F_b [N]	G [10^{-3} J/mm ²]	K [N/mm ^{3/2}]	K [MPa \sqrt{m}]
1	40	1180	0.08	8.70	0.28
2	40	1154	0.08	8.51	0.27
3	40	1196	0.09	8.82	0.28
5	40	1124	0.08	8.28	0.26
6	40	1306	0.10	9.63	0.30
7	40	1402	0.12	10.33	0.33
average		1227	0.09	9.04	0.29
Standard deviation		9	23.44	11.51	11.51
[% of average]					

6 Discussion of the results

The photobond 350 and 368 adhesive seem to have low damage tolerance. Even in specimens where the scatter in strength is limited, such as specimen type B, the scatter in fatigue life can be several orders of magnitude. Although fatigue life is increased by lowering the stress amplitude, this does not affect the scatter in the fatigue lives. The adhesives used, seem to have no visco-elastic flow behaviour and therefore fatigue life is not increased by decreasing the frequency. If

anything the decreased frequency increases the fatigue life. Even in tests with very short fatigue lives no damage accumulation per cycle is visible until final failure in the last cycle(s).

Table 6: Results for GB 350 bonded specimens

Specimen number	a_c [mm]	F_b [N]	G [10^{-3} J/mm ²]	K [N/mm ^{3/2}]	K [MPa \sqrt{m}]
1	40+5	1042	0.07	7.68	0.24
2	40+10	1187	0.09	8.75	0.28
4	40+6	1085	0.09	9.20	0.29
5	40+15	700	0.06	7.09	0.22
6	40+17	700	0.06	7.35	0.23
7	40+15	767	0.07	7.77	0.25
8	40+30	500	0.05	6.45	0.20
average		854	0.08	8.21	0.26
st. dev. [% of average]		29	23.44	12.51	12.51

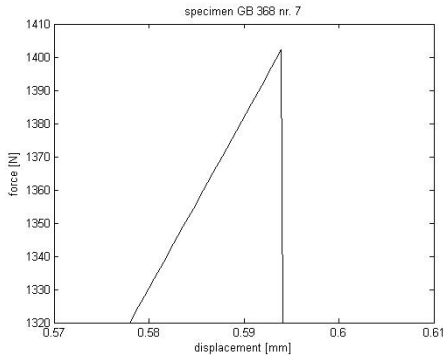


Figure 9: Plot of displacement against force at failure, GB 368, specimen 7

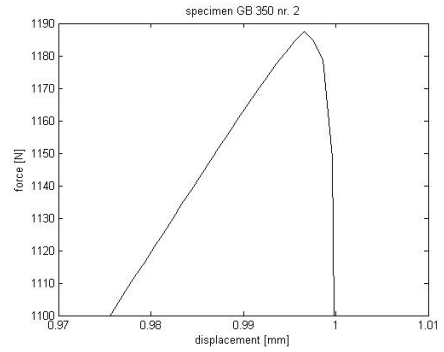


Figure 10: Plot of displacement against force at failure, GB 350, specimen 2

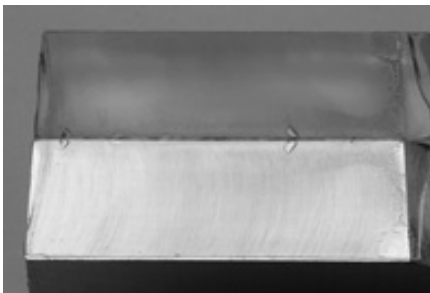


Figure 11: GB 368, specimen 7 topview of bonding surface after failure

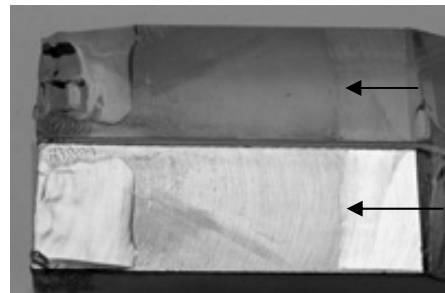


Figure 12: GB 350, specimen 2 surface, topview of bonding surface after failure

Specimen type seems to be less important in reducing the fatigue scatter than previously assumed. An important observation is that reducing the scatter in tensile test results does not seem to reduce the scatter in fatigue life.

For the particular adhesives used, it appears that fatigue testing cannot give any meaningful result. The adhesives do not have a significant increase in damage during fatigue testing as the force displacement diagram shows a constant maximum displacement. Thus the pre-existing damage will be the determining factor in fatigue life. Even the most careful control of the consistency of the application and curing processes does not seem to be able to result in an acceptable scatter in fatigue lives, in contradiction to earlier, tests on more visco-elastic adhesive, [3,6]. This implies that these adhesives are not suitable for fatigue critical joints.

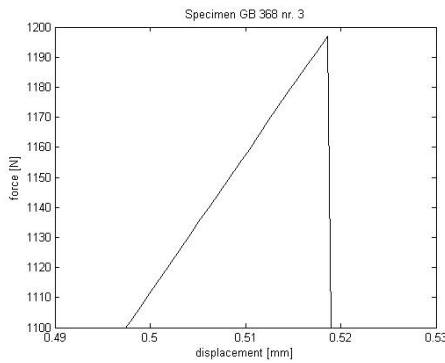


Figure 13: Plot of displacement against force at failure, GB 368 specimen 3

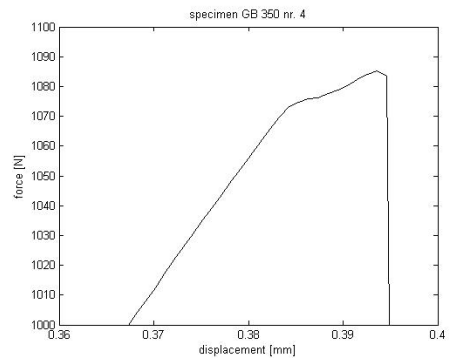


Figure 14: Plot of displacement against force at failure GB 350 specimen 4

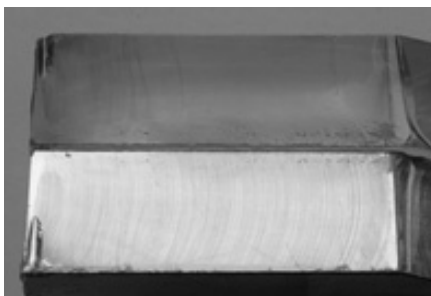


Figure 15: GB 368, specimen 3 topview of bonding surface after failure

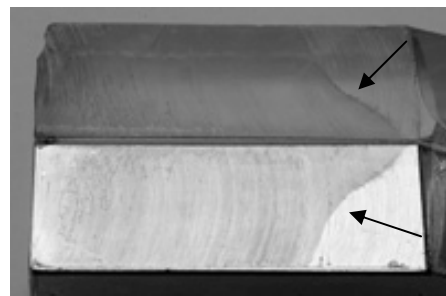


Figure 16: GB 350, specimen 4 topview of bonding surface after failure

When the results of the fracture toughness tests are compared, one can clearly see the differences in fracture behaviour. The fracture behaviour of 368 is very brittle and cohesion based. In contrary to the 368, the 350 shows a tougher fracture behaviour. As can be seen in the photographs in Figures 12 and 16, the fracture surfaces show that the adhesive was peeled from the surface due to adhesive failure. In most cases this occurred prior to instability. Peeling is very detrimental for the strength of bonded joints as it is a permanent damage and can cause serious problems due to increased corrosive attack by moisture and contaminants. Also, peeling takes place at a significantly lower load level. In this context, when comparing the adhesives under a mode I loading, the joint bonded with GB 350 is weaker than the one bonded with GB 368. The fracture toughness of materials can only be determined if a crack is present and failure originates from this crack. Although crack initiation was difficult to check and peeling was dominant for GB 350, an estimate for K_C was made in Tables 5 and 6 based on the test results. Both G and K values are in the same order of magnitude for both types of adhesive. The values confirm the brittle fracture behaviour as was seen in the load displacement curves.

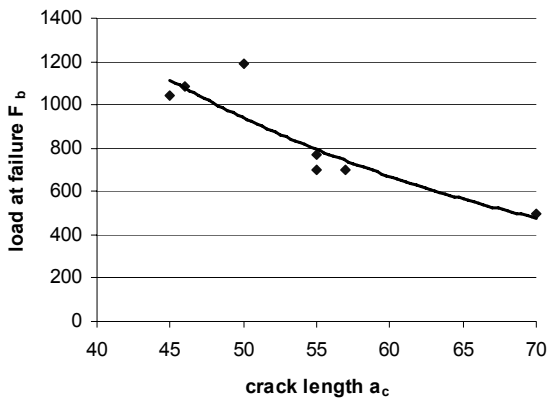


Figure 17: GB 350 relation load at failure to crack length

The obtained K_C values for GB 350 describe the toughness of the adhesion of the adhesive, rather than the cohesion. Figure 17 shows that there certainly is a relation between the crack length (peel length) and the load at failure. The only exceptional result is that of specimen 2. Figure 12 reveals that peeling takes place at first. Then, the adhesive cracks and stable crack growth continues until the combination of crack length and stress reaches a critical level, resulting in failure. This type of failure gives better results in terms of K_C , but is not common.

7 Conclusions

From the results the following can be concluded:

- The GB 350 and GB 368 adhesives do not have any significant visco-elastic flow in fatigue tests
- The fatigue life seems to be increased with decreasing frequency
- The GB 350 and GB 368 adhesives have a low damage tolerance
- As a result of the low damage tolerance both adhesives are extremely sensitive to damage introduced during manufacturing
- The choice of specimen can influence the scatter in tensile tests
- The choice of specimen has at best only a secondary effect on the scatter in fatigue tests
- The GB 350 has better tensile results, but the fatigue and fracture toughness results are worse than GB 368

The purpose for this research was to compare the originally used photobond (GB 368) for the ATP with the recommended photobond (GB 350), a rubber modified version of the GB 368 which should be more resistant to impact loading. The results of the three tests (tensile, low cycle fatigue and fracture toughness) show a difference, but it's not the intended improvement. The modification is insufficient to obtain better performances and moreover creates another problem in peel strength. Due to peeling, the GB 350 is more likely susceptible to the negative effects of corrosion by moisture and contaminants. Although useful information about the fracture behaviour of the adhesives has been obtained, in this stage further research has to be performed in order to map other important characteristics of the adhesives, such as fire resistance. Information about several characteristics of the adhesives, following from results of various tests should give a more complete view on the (im)possibilities so that both adhesives can be applied for the right situation.

References

- [1] F. Bos, F.A. Veer, G. Hobbelman, T. Romein, R. Nijse, J. Belis, P.C. Louter, E. van Nieuwenhuijzen 'Designing and Planning the World's Biggest Experimental Glass Structure' Conference Glass Processing Days, Finland, 2005
- [2] F.A. Veer, M.J.H.C. Jansen, T. Nägele, 'The possibilities of glass bond adhesives', Conference Glass Processing Days, Finland, 2005

- [3] F.A. Veer and J. Zuidema, 'The relationship between adhesive application and fatigue lifetime for a photocatalytic adhesive joint.' To be published in the international journal for adhesion and adhesive in 2007.
- [4] www.delo.de
- [5] A.C. Riemsdag 'Crack growth in polyethylene', PhD Thesis Delft University of Technology, 1997
- [6] F.A.Veer, J.Schönwälder, J.Zuidema, C. van Kranenburg 'Failure criteria for transparent acrylic adhesive joints under static, fatigue and creep loading' Proceedings ECF 15 conference Stockholm 2004
- [7] ASTM E399-05 Standard Test Method for Linear-Elastic Plane-Strain Fracture Toughness K_{Ic} of Metallic Materials

